J. Phys.: Condens. Matter **12** (2000) 3131–3148. Printed in the UK PII: S0953-8984(00)10414-X

Annealing of α-decay damage in zircon: a Raman spectroscopic study

Ming Zhang†, Ekhard K H Salje†, Gian Carlo Capitani‡, Hugues Leroux‡, Andrew M Clark§, Jochen Schlüter‖ and Rodney C Ewing¶

† Department of Earth Sciences, University of Cambridge, Downing Street, Cambridge CB2 3EQ, UK
‡ Laboratoire de Structure et Propriétés de l'Etat Solide, Bâtiment C6, Université Sciences et Technologies de Lille, 59655 Villeneuve d'Ascq, France
§ Department of Mineralogy, The Natural History Museum, Cromwell Road, London SW7 5BD, UK
‖ Mineralogisches Museum, Mineralogisch-Petrographisches Institut, Universität Hamburg, Grindelallee 48, D-20146 Hamburg, Germany
¶ Department of Nuclear Engineering and Radiological Sciences Department of Geological Sciences, University of Michigan, Ann Arbor, MI 48109-2104, USA

E-mail: mz10001@esc.cam.ac.uk (M Zhang)

Received 16 December 1999

Abstract. Recrystallization and structural recovery in α-decay damage in zircon samples have been studied using Raman spectroscopy. Fifteen zircon samples with different degrees of radiation damage have been thermally annealed between 600 K and 1800 K for up to 28 days and 8 hours. The experimental results from this study reveal that recrystallization in the damaged zircon samples is a multi-stage process that depends on the degree of initial damage of the samples. In partially damaged samples the lattice recovery of damaged crystalline $ZrSiO_4$ takes place at temperatures as low as about 700 K, as shown by a remarkable band-sharpening and a significant increase in the frequencies of ν_1 and ν_3 Si–O stretching vibrations together with the external band near 357 cm^{-1} with increasing temperature. A dramatic increase of Raman scattering intensity of $ZrSiO_4$ occurs in partially damaged samples near 1000 K due to a recrystallization process involving epitaxial growth. Heavily damaged samples tend to decompose into ZrO_2 and SiO_2 at high temperatures. Tetragonal ZrO_2 has been observed under annealing between 1125 K and about 1600 K in heavily damaged samples while monoclinic ZrO_2 appears above 1600 K. Weak signals from $ZrSiO_4$ were detected at 1125 K in highly metamict zircon although the main recrystallization appears to occur near 1500 K accompanied by a decrease of the volumes of ZrO_2 as well as SiO_2. This suggests that this recrystallization is associated with the reaction of ZrO_2 with SiO_2 to form $ZrSiO_4$.

A possible intermediate phase has been observed, for the first time, by Raman spectroscopy in damaged zircons annealed at temperatures between 800 K and 1400 K. This phase is characterized by strong, broad Raman signals near 670, 798 and 1175 cm^{-1}. Prolonged isothermal annealing at 1050 K results in a decrease of these characteristic bands and eventually the disappearance of this intermediate phase.

1. Introduction

Zircon ($ZrSiO_4$) is widely used in the ceramic, foundry and refractory industries. It has also been proposed as a waste form for the disposal of plutonium from dismantled nuclear weapons (Burakov 1993, Anderson *et al* 1993, Ewing *et al* 1995, Weber *et al* 1996, Ewing 1999). Self-radiation damage from α-decay of the incorporated actinides can affect the durability and

0953-8984/00/133131+18$30.00

performance of these actinide-bearing phases. The evaluation of the effect of radiation on the crystalline phase and understanding of the damage and recrystallization mechanisms and the structure of the damaged phase are one of the critical concerns for this application.

Zircon is tetragonal ($I4_1/amd$ and $Z = 4$) (Hazen and Finger 1979). The ideal structure consists of a chain of alternating, edge-sharing SiO_4 tetrahedra and ZrO_8 triangular dodecahedra extending parallel to the crystallographic c-axis. Natural zircons are commonly found with U and Th, as well as other rare earth elements. Due to radioactive decay of naturally occurring radionuclides and their daughter products in the ^{238}U, ^{235}U and ^{232}Th decay series the structure of zircon can become heavily damaged over geological time. As a result, natural zircon is commonly found in the 'metamict' state, an aperiodic or amorphous state caused by α-decay radiation damage (Ewing 1994).

Annealing of metamict zircon is typically done in order to restore the original crystal structure for the purpose of phase identification and to gain an understanding of the recrystallization mechanism. Previous investigations (Stott and Hilliard 1946, Vaz and Senftle 1971, Vance and Anderson 1972, Mursic *et al* 1992a, Weber 1991, 1993, Ellsworth *et al* 1994, Farges 1994, McLaren *et al* 1994, Jaeger *et al* 1997, Colombo and Chrosch 1998a, b, Meldrum *et al* 1998, Colombo *et al* 1999, Begg *et al* 2000, Capitani *et al* 2000) elucidated some aspects of the mechanism and kinetics of recrystallization of metamict zircon although several issues are still not clear.

Firstly, what happens at an atomic level during high temperature annealing is not known and even the local structure of metamict zircon remains elusive. Based on density and XRD measurements, Weber (1991, 1993) reported a two-stage recovery in Pu-doped zircon annealed at high temperatures. The author suggested that the first-stage recovery, appearing near 1323 K, was related to decomposition of damaged zircon and the second-stage recovery was associated with the transformation back to the original $ZrSiO_4$ crystal structure at a higher temperature (the author could not determine exactly when recrystallization to $ZrSiO_4$ structure started due to the uncertainty in the XRD data). An *in situ* single-crystal neutron diffraction study on partially metamict zircon samples up to 2000 K by Mursic *et al* (1992a) showed that for untreated metamict samples the probability density function of the oxygen atoms exhibited minima in directions towards Zr and Si atoms, but for samples annealed at 1573 K and 1873 K the minima disappeared and there was an increased density shift towards the Si atoms. These authors suggested that the observed recrystallization of the damaged zircon could be related to a structural relaxation at high temperatures which was seen in a synthetic sample (Mursic *et al* 1992b). Farges (1994) reported that XRD data showed a decrease of the cell parameter a from 6.674 Å at 573 K to 6.610 Å at 873 K for a damaged zircon and Zr-K EXAFS analysis indicated a progressive (VII) Zr⇒ (VIII) Zr transition, associated with a recovery of the crystalline zircon medium-range environment at higher temperatures (approximately between 927 K and 1273 K).

Secondly, although it has been generally agreed that highly metamict zircon tends to decompose into ZrO_2 and SiO_2 at high temperatures, different polymorphs of ZrO_2 have been reported in different studies. In a thermal anneal study using x-rays, Vance and Anderson (1972) reported cubic and tetragonal ZrO_2 at 1073 K and 1373 K, respectively. Farges (1994) reported monoclinic ZrO_2 in heavily damaged samples heated to 1373 K. McLaren *et al* (1994) observed, in heavily damaged zircon with high uranium content, that annealing at 1173 K produced randomly orientated ZrO_2 crystallites of roughly 10 nm size while annealing at 1523 K produced baddeleyite crystals (monoclinic ZrO_2) of 1000 nm dimensions and an easily identifiable silica glass phase in the regions that were initially optically isotropic. Ellsworth *et al* (1994) observed crystalline ZrO_2 in heavily damaged zircon annealed at 1273 K. Due to its broad x-ray diffraction peaks, these authors could not determine whether it was cubic or

tetragonal. Ellsworth *et al* (1994) also pointed out that decomposition of metamict zircon into ZrO_2 and SiO_2 could be one possible path for recrystallization. An x-ray powder diffraction study at high temperature (Colombo and Chrosch 1998b) reported the appearance of pseudo-cubic ZrO_2. Meldrum *et al* (1998) observed a decomposition of zircon into tetragonal ZrO_2 when irradiating zircon with heavy ions at around 950 K.

Finally, there are some experimental results suggesting that zircon samples with different degrees of damage show different recovery behaviours. A thermoluminescence study by Vaz and Senftle (1971) showed that heating samples with different degrees of α-decay damage to 1223 K for 20 h in N_2 atmosphere resulted in an increase in signals of zircon, but the increase in terms of light output was α-dose dependent. Ellsworth *et al* (1994) reported that the enthalpy (relative to crystalline zircon) of annealing varied sigmoidally as a function of radiation dose and it reached a saturation plateau (-59 ± 3 kJ mol^{-1}) at radiation dose greater than 5×10^{18} α-events g^{-1}. A recent study using time-differential perturbed angular correlation spectroscopy (Jaeger *et al* 1997) showed that at some temperatures the degree of recovery was related to the degree of the initial damage of the sample.

We undertook this study to understand the mechanism and kinetics of recrystallization and structural recovery of metamict zircon on annealing. Raman spectroscopy was used because it has a correlation length scale of about a few unit cells and it has been widely used in the study of amorphous and nanometric materials and ZrO_2 (Siu *et al* 1999, Zhang *et al* 2000). We shall show in later sections that recrystallization in zircon is strongly dose dependent and heavily damaged zircon samples exhibit a more complex recrystallization path than weakly damaged zircon samples. Heating heavily damaged samples to high temperatures can lead to the appearance of tetragonal and monoclinic ZrO_2 and unavoidable SiO_2 phases. We shall also report experimental data showing the existence of a possible intermediate phase occurring during annealing at temperatures above 800 K.

2. Experiment

The samples used in this study were analysed using electron microprobe, x-ray and infrared spectroscopy. Seven of them have been previously studied by Murakami *et al* (1991), Salje *et al* (1999) and Zhang *et al* (2000). The lattice parameters of some of the samples were determined by x-ray Guinier powder diffraction with Si as internal standards. Electron microprobe analysis was performed on polished thin sections of zircon samples using a Cameca SX5D electron microprobe with a Link AN10000 energy-dispersive spectrometer. A beam size of 5 μm was used with a beam current of 100 nA. Tables 1 and 2 list the details. According to x-ray diffraction patterns, unit cell parameters, infrared and Raman spectra, samples Vigene, Moroto, Miass, Green River, UG13, Henderson and 269 are undamaged or slightly damaged (with estimated dose of less than 2×10^{18} α-events g^{-1}); samples Cam26, Cam10 and 4604 have intermediate degrees of damage (between 2 and 3.5×10^{18} α-events g^{-1}); samples Cam27, Ni12 and Z3 are heavily damaged with dose between 5.6 and 7.9×10^{18} α-events g^{-1}; samples 157 (with dose of 13.1×10^{18} α-events g^{-1}) and Sd4 (15.9×10^{18} α-events g^{-1}) are highly metamict. All annealing experiments were carried out in N_2 atmosphere in a vertical furnace. Annealed samples were quenched in air.

Raman spectra were recorded at room temperature using a Bruker IFS 66v spectrometer adapted with a Bruker FRA 106 FT–Raman accessory. A silicon-coated calcium fluoride beam-splitter and radiation of 1064 nm from an Nd:YAG laser were used for the excitation laser which can produce 350 mW output. A liquid-nitrogen-cooled, high sensitivity Ge detector was used. The spectra were recorded with a laser power of 45–100 mW and a back scattering geometry. The focused beam was about 200 μm in size. For crystalline zircon samples 250–512 scans

Table 1. Zircon sample descriptions. Dosage is in units of 10^{18} α-events g^{-1}.

Zircon	Locality	Dose	a (Å)	c (Å)	V (Å^3)	Reference/source
Vigene	unknown	ND	6.6053	5.9802	260.96	unknown
Moroto	Uganda	ND	6.6056	5.9834	261.08	Peter Leggo
Miass	Miass, Urals, Russia	ND	6.6066	5.9813	261.06	NHM
Green River	North Carolina, USA	ND	6.6055	5.9827	261.04	NHM
UG13	Uganda	ND	6.6106	5.9943	261.95	Peter Leggo
Henderson	North Carolina, USA	ND	6.6156	6.0076	262.93	NHM
269	Sri Lanka	1.8	6.6301	6.0266	264.91	Zhang *et al* (2000)
Cam26	Sri Lanka	2.9		ND		Zhang *et al* (2000)
Cam10	New York, USA	ND	6.6394	6.0549	266.91	CAM
4604[a]	Sri Lanka	3.5	6.68	6.07	271	Murakami *et al* (1991)
Cam27	Sri Lanka	5.6		ND		Zhang *et al* (2000)
Ni12	Sri Lanka	7.1		ND		Zhang *et al* (2000)
Z3	Sri Lanka	7.6		unable to determine a and c		HAM
157	Sri Lanka	13.1		ND		Zhang *et al* (2000)
Sd4	Sri Lanka	15.9		ND		Zhang *et al* (2000)

ND = not determined.
[a] Measured by Murakami *et al* (1991).
CAM = Sedgewick Museum, University of Cambridge, UK; HAM = Mineralogisches Museum, Mineralogisch-Petrographisches, Universität Hamburg, Germany; NHM = Natural History Museum, UK; 269 = BM1920,269; 157 = BM1921,157.

Table 2. Electron microprobe analyses of zircon samples.

Sample	SiO_2	FeO	ZrO_2	HfO_2	CaO	Al_2O_3	Y_2O_3	ThO_2	UO_2	Total
Vigene	33.39	—	66.59	0.86	—	—	0.03	0.01	0.01	100.89
Moroto	31.37	—	65.64	1.28	0.01	0.01	0.01	0.01	0.02	98.34
Miass	32.01	—	65.84	1.11	—	0.01	0.14	0.02	0.04	99.17
UG13	30.73	0.01	65.63	1.69	0.01	0.02	0.08	0.01	0.11	98.29
Henderson	32.81	0.04	66.12	0.92	—	0.01	0.37	0.44	0.13	100.84
Green River	32.62	0.01	65.89	0.96	—	0.01	0.06	0.07	0.07	99.68
Cam26	33.36	0.01	65.26	1.28	0.01	—	0.03	0.03	0.18	100.16
Cam10	32.70	0.01	64.84	1.92	—	—	0.15	0.03	0.24	99.89
4604	32.04	0.02	66.51	1.27	—	—	0.10	0.08	0.32	100.34
Cam27	33.38	—	63.26	2.81	0.01	—	0.22	0.05	0.36	100.09
Ni12	32.68	—	65.74	1.64	—	0.01	0.02	0.14	0.39	100.62
Z3	32.87	0.01	65.82	2.19	0.01	0.01	0.12	0.09	0.49	101.61
157	32.48	0.01	64.85	2.36	0.05	—	0.10	0.08	0.86	100.79
Sd4	32.69	0.01	65.66	0.63	—	0.01	0.01	0.12	1.02	100.15

— Undetectable.

were used and 1000–3000 scans for heavily damaged samples. The resolution of all the spectra was 2 cm^{-1}.

3. Results

Nine of the 12 predicted Raman modes ($2A_{1g} + 4B_{1g} + B_{2g} + 5E_g$, Dawson *et al* 1971) were observed in untreated crystalline zircon samples (e.g. samples Vigene, Moroto and Miass), and our results are consistent with previously reported Raman data (Dawson *et al* 1971, Nicola and Rutt 1974, Syme *et al* 1977, Nasdala *et al* 1995, Hoskin and Rodgers 1996, Zhang *et al* 2000). They are internal modes: 1008 cm^{-1} (B_{1g}, Si–O ν_3 stretching), 975 cm^{-1} (A_{1g}, Si–O

ν_1 stretching), 439 cm^{-1} (A_{1g}, Si–O ν_2 bending), and 269 cm^{-1} (B_{2g}, Si–O ν_2 bending) and external modes: 393, 355, 225, 214 and 202 cm^{-1} (Syme *et al* 1977, Hoskin and Rodgers 1996). The other predicted bands are too weak to useful for this study.

3.1. Effects of annealing temperature

Raman spectra of zircon samples with different degrees of α-decay damage annealed at different temperatures for 1 h are shown in figure 1. Thermal annealing reveals different recrystallization processes between partially and heavily damaged samples, i.e. the recrystallization process depends on the cumulative radiation dose. We shall describe the spectral variations due to thermal treatment separately for partially damaged samples and heavily damaged ones.

With increasing annealing temperature, slightly damaged samples (Moroto, Miass, Vigene, Henderson, Green River and UG13), and weakly damaged samples (269 and 4604) show a weak increase of Raman band intensity between 800 K and 1000 K (figure 1). Dramatic changes of intensity are observed in the samples annealed between 1000 and 1100 K. An increase of Raman intensity in the region below 300 cm^{-1} tends to occur between 800 and 900 K in some partially damaged samples, e.g. 4604 (figure 1). For some crystalline zircon samples, e.g. Miass, Henderson and Green River, thermal annealing between 1600 and 1800 K causes a decrease of intensity in their Raman signals of crystalline $ZrSiO_4$. This may be due to slight decomposition into monoclinic ZrO_2 at these temperatures although no ZrO_2 was detected.

For heavily damaged samples (e.g. Ni12, Z3, 157 and Sd4), no significant variations of spectral features were seen between 300 K and 800 K (figure 1). In the samples annealed at 900 K, extra spectral features appear near 670, 798 and 1175 cm^{-1}. However, these spectral features become weaker in intensity with increasing annealing temperature and could not be traced at temperatures above 1400 K. Apart from these additional signals, tetragonal ZrO_2 was observed in heavily damaged samples (e.g. at 1125 K, 1150 K and 1175 K for sample Sd4 and at 1200 K, 1300 K, 1400 K and 1500 K for sample 157) while monoclinic ZrO_2 was seen above 1600 K in samples Z3 and Ni12 (figure 1).

The effect of annealing temperature on the structural recovery of damaged zircon can also be clearly seen in the frequency of the ν_3 Si–O stretching (the band was assigned as B_{1g} by Syme *et al* (1977) and Hoskin and Rodgers (1996)) as a function of temperature (figure 2(a)). With increasing annealing temperature the frequency of this mode shows, systematically, a large increase with temperature in the region between 800 K and 1050 K and a weaker increase with temperature above 1050 K. Apart from this vibration, the internal Si–O stretching mode near 975 cm^{-1} (ν_1, A_{1g}) and the external mode near 356 cm^{-1} (E_g) also show an increase of frequency with temperature (figure 2(b)). In contrast, the frequency of the Si–O bending near 438 cm^{-1} (ν_2, A_{1g}) seems almost unaffected by thermal annealing. The other external modes below 300 cm^{-1} are so weak that we did not attempt to determine the temperature dependence of their frequencies.

3.2. Effects of annealing time

In order to understand the effects of annealing time on the recrystallization process in radiation-damaged zircon samples, weakly damaged sample UG13 was annealed for 2 h between 600 K and 1700 K with a temperature interval of 100 K. Raman spectra of the annealed sample show a similar temperature evolution to that of samples (e.g. sample 269) with a similar degree of damage, following annealing for 1 h.

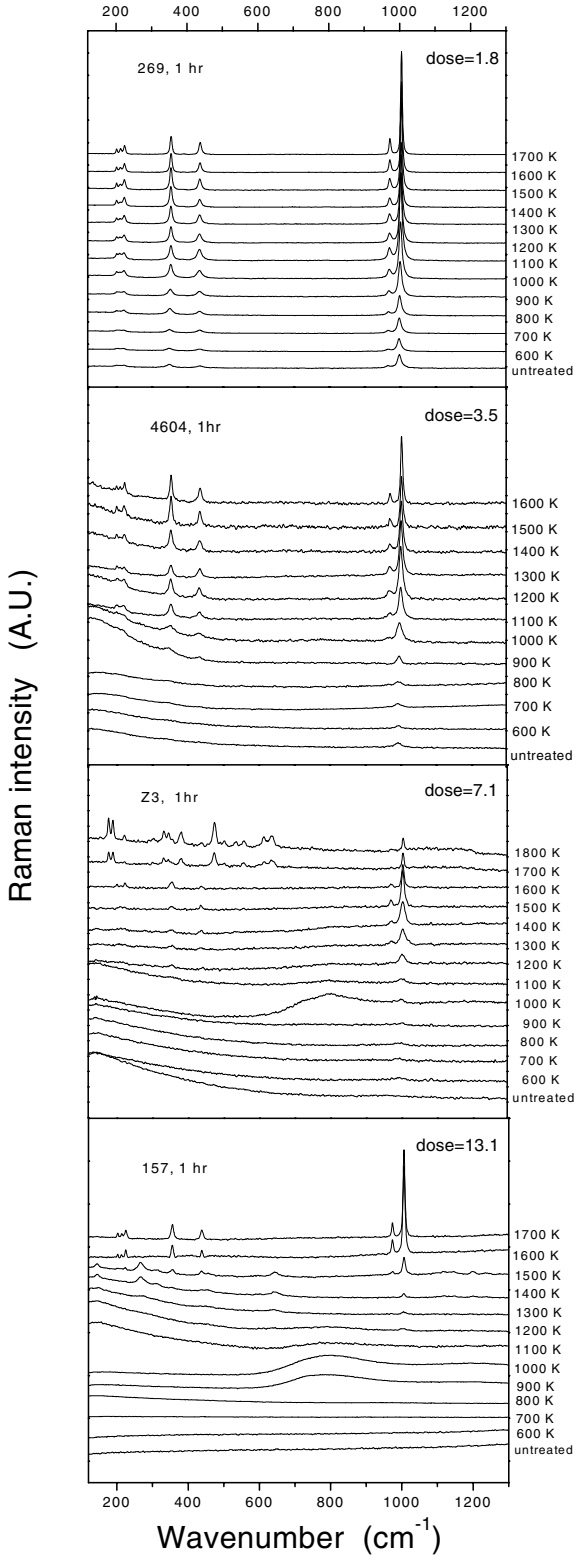

Figure 1. Temperature evolution of Raman spectra of zircon samples with different degrees of radiation damage between 120 and 1300 cm^{-1}. Dosage is in units of 10^{18} α-events g^{-1}. Samples are annealed for one hour at the designed temperature and then measured before further annealing at a higher temperature.

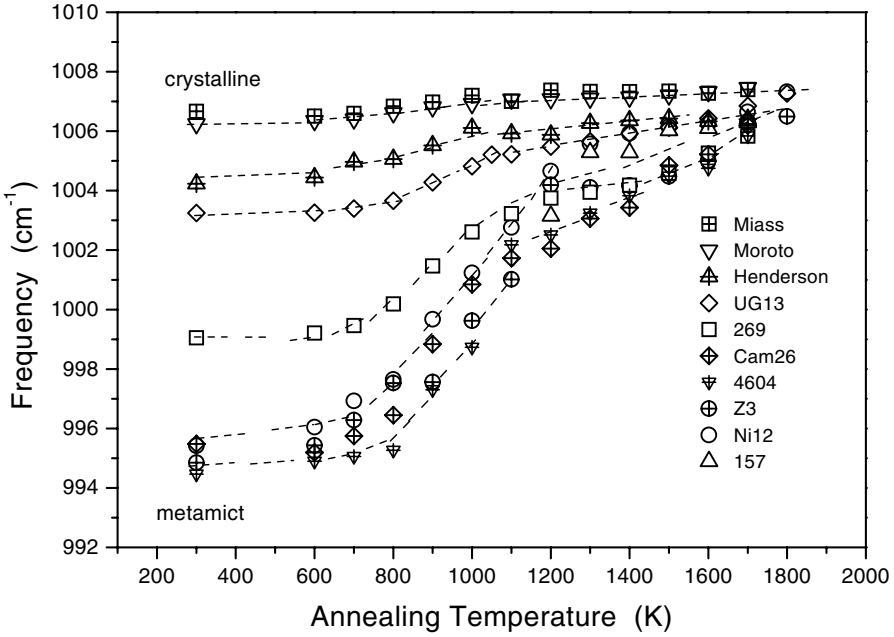

(a)

Figure 2. Phonon frequencies as a function of annealing temperature. (a) ν_3 Si–O stretching; (b) external and internal modes for sample 269. All the samples were annealed for 1 h except UG13 (2 h) and Cam26 (16 h).

The more significantly damaged samples from zircon Cam26, Cam27 and 157 were annealed for 16 h. These showed similar spectral features to samples annealed for 1 h except in the temperature region between 900 K and 1300 K (figure 1 and figure 3). In this temperature region the additional bands near 670, 798 and 1175 cm^{-1} can hardly be detected in Cam26 (dose $= 2.9 \times 10^{18}$ α-events g^{-1}) and Cam27 (dose $= 5.6 \times 10^{18}$ α-events g^{-1}) while they appear as very weak features in a sample from zircon 157 (dose $= 13.1 \times 10^{18}$ α-events g^{-1}) annealed at 1000 K.

In order to understand why the extra signals are absent or too weak to be detected in long-time annealed samples, samples UG13 and Cam10 were isothermally annealed at 1050 K up to 22 days and 8 hours (figures 4(a) and 4(b)). We find that the time dependence of the Raman spectra of damaged zircon is also affected by the initial degree of damage. The weakly damaged zircon UG13 (1.6×10^{18} α-events g^{-1} which is estimated using the dose–linewidth and dose–frequency dependences reported by Zhang *et al* (2000) due to the lack of the information on its geological age) shows weak changes in Raman intensity, peak frequency and width (figures 4(a) and 5) with increasing annealing time. However the more significantly damaged zircon Cam10 (estimated dose $= 4.2 \times 10^{18}$ α-events g^{-1}) shows much stronger spectral variations with increasing annealing time. For the case of short annealing time, extra signals located between 500 and 800 cm^{-1} and near 1175 cm^{-1} were observed in Cam10 (figure 4(b)) and they exhibit a significant decrease in intensity with increasing annealing time. The Raman spectra of Cam10 in figure 4(b) were normalized against the height of the ν_3 Si–O stretching mode to show the relative change of intensity for these extra signals with increasing anneal time. These extra signals become very weak in Cam10 annealed for 16 h and they can be hardly traced in the spectra of Cam10 annealed for 72 h and 536 h. These additional signals

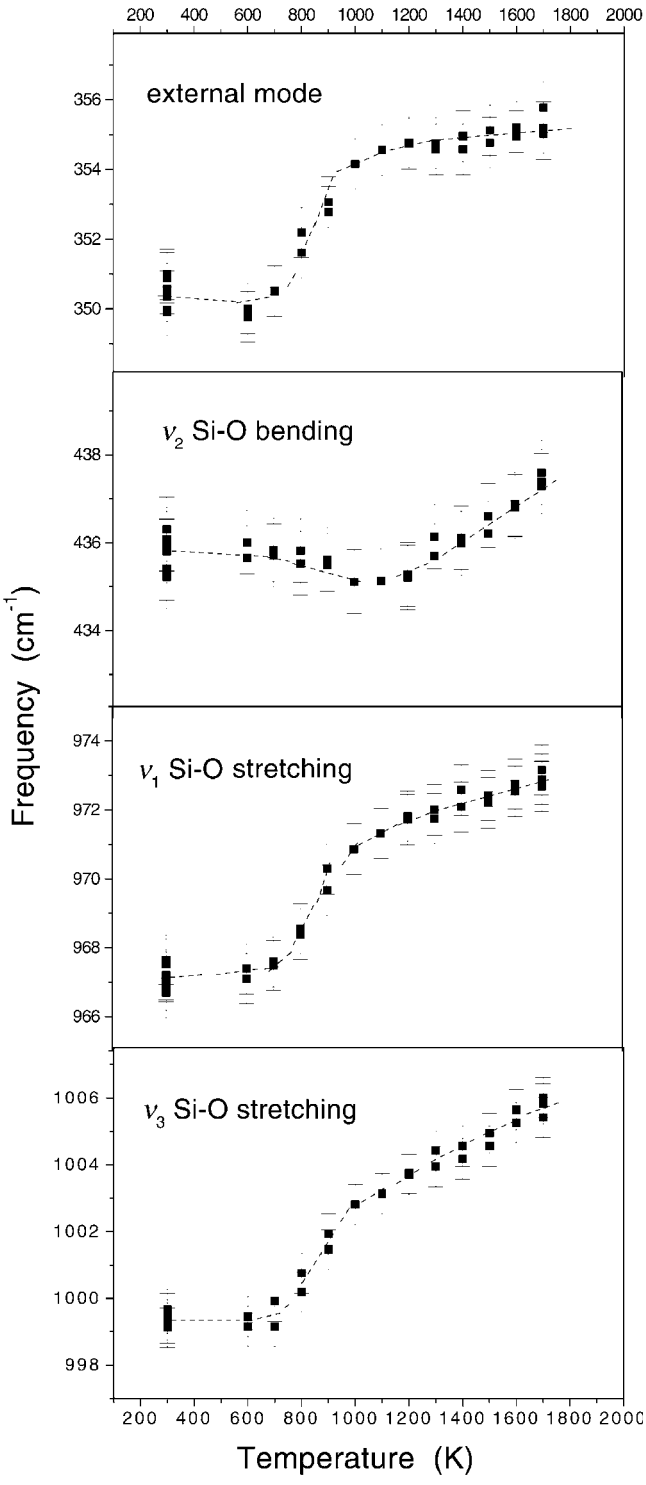

(b)

Figure 2. (Continued)

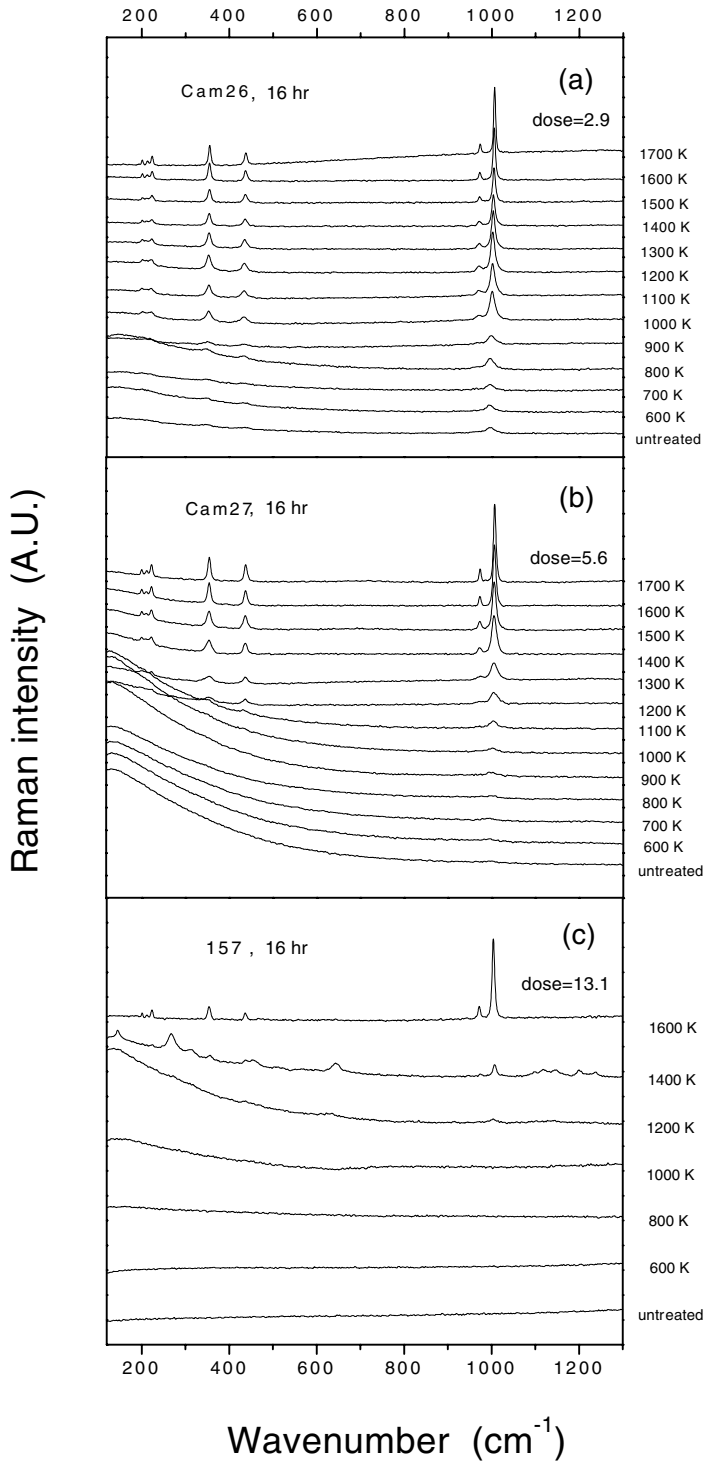

Figure 3. Temperature evolution of Raman spectra between 120 and 1300 cm^{-1} of zircons annealed for 16 h. (a) Cam26; (b) Cam27; (c) 157. Fresh samples were annealed at each temperature. Dosage is in units of 10^{18} α-events g^{-1}.

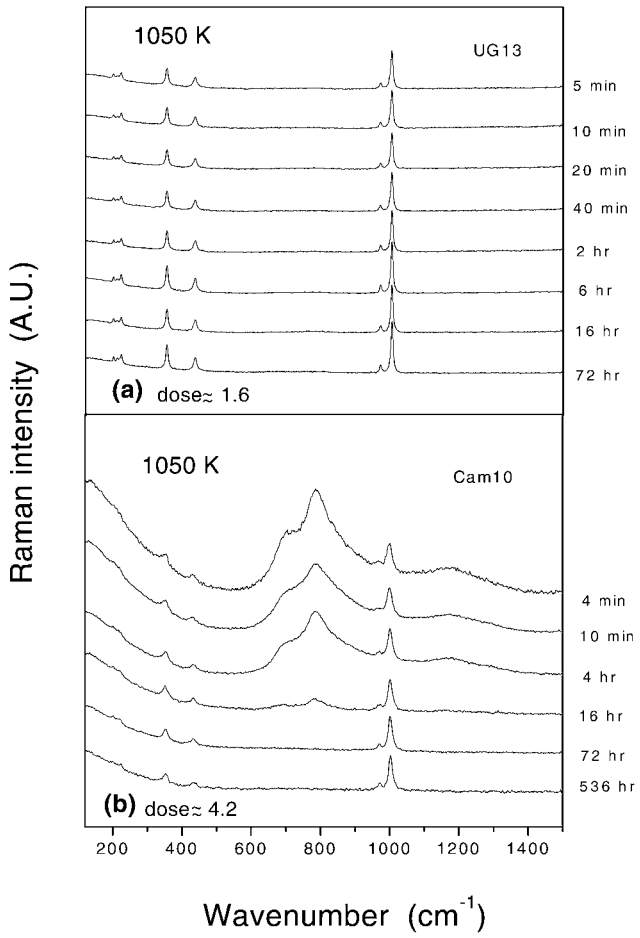

Figure 4. Time evolution of Raman spectra between 120 and 1500 cm^{-1} (annealing temperature = 1050 K). (a) UG13; (b) Cam10. For the case of (b), the Raman spectra are normalized by the height of the Si–O stretching band near 1007 cm^{-1} to show the detailed spectral changes. Fresh samples were annealed.

could indicate an intermediate phase which starts to appear between 800 K and 900 K and it tends to disappear above 1400 K or during prolonged annealing.

A crystal from sample 157 was annealed at 1100 K for 21 days. The annealed sample did not show any detectable crystalline $ZrSiO_4$. A crystal of sample 157 annealed at 1400 K for 16 h shows sharper Raman lines of crystalline $ZrSiO_4$ than those samples annealed at the same temperature for 1 h and a higher intensity of Si–O stretching ν_3 of $ZrSiO_4$ relative to that of the 643 cm^{-1} Zr–O band of tetragonal ZrO_2.

3.3. ZrO_2 and SiO_2

Zirconia has three common polymorphs: the monoclinic, tetragonal and cubic phase (Smith and Newkirk 1965). The different polymorphs of ZrO_2 can be distinguished by Raman and infrared spectroscopy. Factor-group analysis predicts the irreducible representations of optical phonons (for zero wave vector) for each polymorph of zirconia ZrO_2 (Keramidas and White

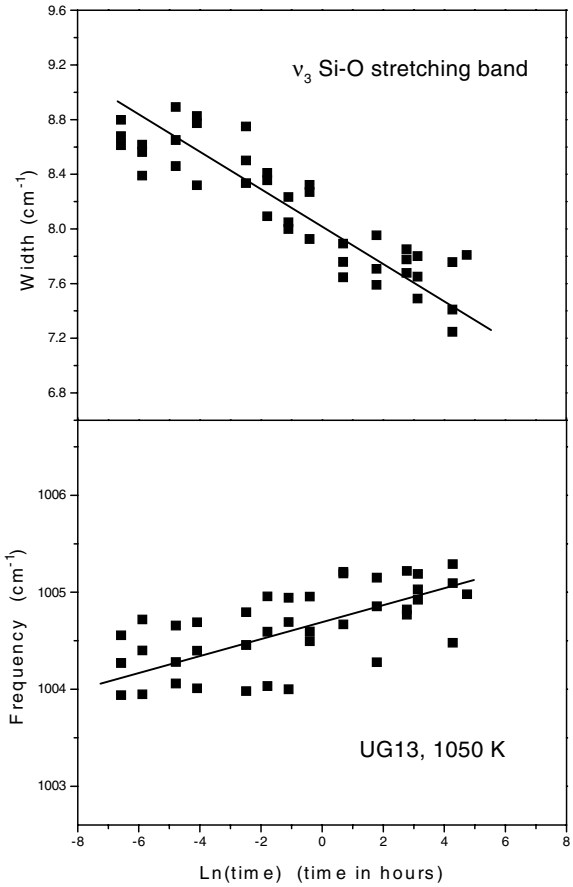

Figure 5. Phonon frequency and width of the ν_3 Si–O stretching for sample UG13 (isothermally annealed at 1050 K) as a function of the natural logarithm of time in hours. The lines are visual guides.

1974, Anastassakis *et al* 1975). For monoclinic ZrO_2 (space group $C^5_{2h}/P2_1/c$, $Z = 4$), 18 modes are expected to be Raman active [$9A_g$ (R) + $9B_g$ (R) + $8A_u$ (IR) + $7B_u$ (IR)]. In tetragonal ZrO_2 with space group $D^{15}_{4h}/P4_2/nmc (Z = 2)$, the predicted representations are A_{1g} (R) + $2B_{1g}$ (R) + $3E_g$ (R) + A_{2u} (IR) + $2E_u$ (IR) and so six phonon modes are expected to be Raman active. For cubic ZrO_2 (space group $O^5_h/Fm3m$, $Z = 1$), the normal modes are F_{2g} (R) + F_{1u} (IR) and only one Raman mode is expected.

No detectable amounts of either oxide were observed in any of the untreated samples used in this study. With annealing up to 1800 K slightly damaged zircon samples (Moroto, Miass, Vigene, Henderson and Green River) do not show ZrO_2 signals. However, thermal treatment of heavily damaged zircon results in the decomposition of metamict $ZrSiO_4$ into ZrO_2 and SiO_2. Extra Raman bands at 144, 266, 312, 453 and 645 cm^{-1} (figures 1, 3 and 6) were recorded in sample 157 (dose = 13.1×10^{18} α-events g^{-1}) annealed at 1200 K. Those signals were also observed in sample Sd4 annealed at 1125 K, 1150 K and 1175 K. Comparing these signals to published data of ZrO_2 (Kim *et al* 1993, Hirata *et al* 1994) shows that these signals are characteristic Raman bands of tetragonal ZrO_2. Tetragonal ZrO_2 could also exist in samples Z3 and Ni12 annealed at 1200 K as their Raman data between 2000 and 3800 cm^{-1}

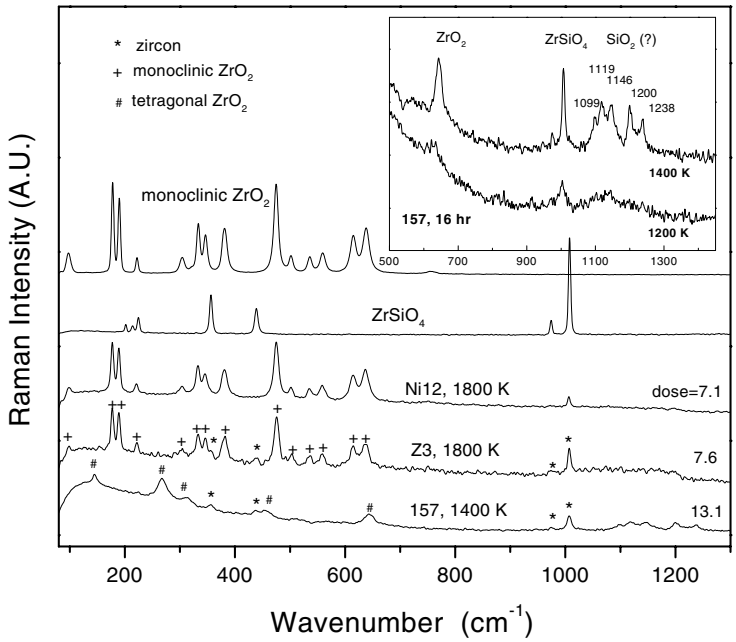

Figure 6. SiO_2 and tetragonal and monoclinic ZrO_2 were observed in heavily damaged zircons annealed at high temperatures. Dosage is in units of 10^{18} α-events g^{-1}. The insert shows five resolved Si–O bands are located at 1099, 1119, 1146, 1200 and 1238 cm^{-1} which are not consistent with SiO_2 glass.

show extra signals which are seen in sample 157 annealed at 1200 K. Fourteen other additional Raman bands at 99, 178, 190, 221, 304, 333, 347, 380, 474, 502, 537, 560, 616 and 638 cm^{-1} together with bands characteristic of zircon are detected in Z3 and Ni12 annealed at above 1600 K (figures 1 and 6). These additional signals match very well with those obtained from a commercial monoclinic zirconia (Alfa, 99.978%) (top in figure 6) and the Raman spectrum of monoclinic zirconia reported by Carlone (1992). Their appearance indicates the existence of monoclinic ZrO_2 in these annealed samples. The volume of monoclinic ZrO_2 in annealed samples may be significantly affected by the quench rate. A crystal of sample Z3 was annealed for 1 h at 1800 K and then allowed to cool slowly to room temperature. This sample did not show significant amounts of monoclinic ZrO_2. Understanding of the impact of quench rate on the decomposition, however, is beyond the objectives of this study.

We saw no evidence of the presence of cubic ZrO_2, which, according to Hirata *et al* (1994), has only one strong characteristic Raman band (F_{2g}) near 607 cm^{-1}, in any of the annealed samples.

Si-rich material must be accompanied by ZrO_2 in order to maintain the original chemical composition of zircon. Such Si-rich phases are correlated with absorption bands between 1000 and 1200 cm^{-1} where Si–O stretching bands from SiO_2 glass are commonly located (figure 6). However, it is striking that the Si-rich phase from sample 157 annealed between 1400 and 1500 K shows five resolved peaks located at 1099, 1119, 1146, 1200 and 1238 cm^{-1}, and these bands are much sharper than those of reported pure SiO_2 glass and silicate glasses (Brawer and White 1975, Mysen *et al* 1980). It is unclear whether the structure of the SiO_2 phase due to the decomposition of metamict zircon has different local structures between 1125 K and 1800 K.

4. Discussion

4.1. Structural recovery in damaged crystalline domains

Samples with intermediate degrees of damage contain crystalline and amorphous domains. Thermal annealing of these samples below 900 K does not produce significant changes in Raman intensities of crystalline zircon (figures 1 and 3). This shows that in this temperature range there is no significant increase in the volume of the crystalline parts implying that the growth of crystalline parts is very slow or absent entirely. This observation is consistent with TEM data from samples Z3 (Capitani *et al* 2000) as well as the work by McLaren *et al* (1994).

The increase in phonon frequencies on annealing in this study is consistent with the Raman observations of metamict zircon reported by Nasdala *et al* (1995) and Zhang *et al* (2000). These authors observed the converse process, i.e. α-decay radiation damage leading to systematic broadening of Raman bands and a significant decrease of Si–O stretching band frequencies reflecting the weakening of the zircon structure and the accumulation of defects. The data from this study also confirm that the observed structural softening in damaged samples by Zhang *et al* (2000) is due to radiation damage rather than chemical impurities. The remarkable variations in Si–O stretching bands during metamictization and thermal annealing are consistent with recent computer simulations of zircon (Williford *et al* 1998) which suggested displacement energy values of 20.4, 90.4 and 53.1 eV for Si, Zr and O, respectively. Our observations also agree with the x-ray work by Farges (1994) who noted a decrease of cell parameter $\boldsymbol{a}$ from 6.674 to 6.610 Å when heating damaged samples from 573 K to 873 K.

It is striking that the temperature dependences of phonon frequencies of zircon show a kink around 1050 K (figure 2). The physical implication of this observation is unclear. Based on a single-crystal neutron diffraction measurement at high temperatures, Mursic *et al* (1992a) proposed that heating a partially damaged zircon to 1250 K could lead to a structural relaxation involving a sudden expansion of Si–O bonds and of SiO_4 tetrahedral volume and allow corner-sharing SiO_4 tetrahedra to rotate. As a result, the strain due to the structural disorder presented in the metamict zircon is released.

The further increase of phonon frequencies and line-sharpening above 1000 K (figures 1 and 2) indicates that the structure of the recovered crystalline domains is still not perfect. In fact, samples annealed at 1500 K show Raman bands that are still broader than those of undamaged samples. This suggests that the temperature required for the full recovery of the crystal structure in damaged zircon must be higher than this temperature for a specimen of zircon with intermediate degrees of radiation damage. Vance (1975) reported a complete recovery of the $ZrSiO_4$ infrared spectrum in severely damaged natural zircon after annealing at 1723 K and Weber (1993) reported that 100% recovery occurred near 1738 K for Pu-doped $ZrSiO_4$.

4.2. Recrystallization and crystal growth

Thermal annealing reveals different recrystallization processes in partially and highly metamict zircon samples. For partially damaged samples, annealing at 1100 K for 1 h results in a significant increase in the intensity of phonon bands of crystalline zircon. It can be understood that the remaining crystalline domains in damaged samples act as seeds for recrystallization. TEM work has shown epitaxial recrystallization in sample Z3 (Capitani *et al* 2000). The existence and growth of these domains might prevent or restrain amorphous parts from decomposition between 1100 K and 1200 K.

Sample 157 annealed at 1100 K for 21 days did not show signals of crystalline $ZrSiO_4$ and ZrO_2, but $ZrSiO_4$ was observed accompanied by tetragonal ZrO_2 in sample 157 annealed at 1200 K for only one hour (figure 1). This observation appears to suggest that the nucleation of crystalline $ZrSiO_4$ in metamict zircon probably occurs between 1100 K and 1200 K. But a very limited number of damaged crystalline $ZrSiO_4$ domains may still exist in such heavily damaged samples (the radiation doses for 157 and Sd4 are 13.1 and 15.9×10^{18} α-events g^{-1}, respectively), and they tend to grow in this temperature region as Salje *et al* (1999) showed that zircon samples with doses as high as 7.2×10^{18} α-events g^{-1} still showed Bragg peaks.

Between 1200 K and 1400 K, sample 157 does not show any significant increase in the Raman intensity of crystalline $ZrSiO_4$, although a weak signal from the ν_3 Si–O stretching vibration was seen at 1200 K. These could be due to the coexistence of ZrO_2, SiO_2 and $ZrSiO_4$ in this sample in this temperature region. The growth of crystalline $ZrSiO_4$ is probably restrained by the presence and the growth of the oxides produced by the decomposition. The main recrystallization in sample 157 occurs near 1500 K, and it is evidenced by the dramatic increase of signals of crystalline zircon accompanied by the disappearance of tetragonal ZrO_2 (figure 1). This suggests that for this highly metamict sample the main recrystallization (near 1500 K) occurs via the reaction of ZrO_2 with SiO_2 in contrast to partially damaged zircon samples in which the remaining crystalline domains play a dominate role in the epitaxial growth near 1000 K.

We have also noted that it is difficult to determine which recrystallization processes are occurring in some heavily damaged samples (e.g. Cam 27, Ni12 and Z3; with doses of 5.6–7.1 $\times 10^{18}$ α-events g^{-1}) (see figures 1 and 3). These two different growth mechanisms probably take place simultaneously, but the decomposition into ZrO_2 and SiO_2 and the appearance of the intermediate phase with characteristic bands near 670, 798 and 1175 cm^{-1} complicate the analysis of the recrystallization process.

4.3. Decomposition of $ZrSiO_4$ into ZrO_2 and SiO_2

In a comprehensive study using x-ray diffraction, infrared, near infrared and visible spectroscopy, Vance (1975) did not observe ZrO_2 in untreated zircon samples and ZrO_2 was recorded in only heated samples. Based on x-ray observation of crystalline ZrO_2 in two heated samples, Ellsworth *et al* (1994) suspected the SiO_2–ZrO_2 unmixing had occurred in the starting metamict zircon. Zhang *et al* (2000) reported that ZrO_2 and SiO_2 are not the principal products of metamictization (but they could not rule out the existence of a small amount of ZrO_2 in natural samples due to experimental resolution). The results from our study suggest that ZrO_2 and SiO_2, as well as an intermediate phase, can occur when damaged samples are heated to high temperatures. Furthermore, our data show that decomposition is more likely to happen in heavily damaged zircon.

Our observation of ZrO_2 is consistent with the observations reported by Weber (1991), Ellsworth *et al* (1994) and McLaren *et al* (1994). In x-ray diffraction data of zircon samples heated up to 1273 K, Ellsworth *et al* (1994) did not detect crystalline ZrO_2 in eight partially damaged samples with doses ranging from 0.061 up to 6.8×10^{18} α-events g^{-1}, but one sample with dose of 7.2×10^{18} α-events g^{-1} showed two phases after annealing, both zircon and ZrO_2. In a more damaged sample (with dose of 11.7×10^{18} α-events g^{-1}) heated to 1273 K, only ZrO_2 was seen in the diffraction pattern by Ellsworth *et al* (1994). Our results further support the observations of Ellsworth *et al* that more heavily damaged samples tend to decompose at high temperatures. The x-ray diffraction peaks were so broad that Ellsworth *et al* (1994) were unable to determine whether the ZrO_2 was tetragonal or cubic. Our results also demonstrate that different ZrO_2 polymorphs can be easily determined using Raman spectroscopy.

It was reported by Meldrum *et al* (1998) that irradiating synthetic zircon with heavy ions at round 950 K led to the appearance of tetragonal ZrO_2, and the authors explained that the observed decomposition of zircon into ZrO_2 and SiO_2 was due to heavy-ion irradiation rather than heating. However, our results show that heating alone can produce an unknown intermediate phase around 900 K while tetragonal ZrO_2 appears at a higher temperature (the lowest temperature at which we observed tetragonal ZrO_2 is 1125 K in this experiment). Crystalline ZrO_2 has also been observed in annealed natural samples by other workers at temperatures higher than that (950 K) reported by Meldrum *et al* (1998) (e.g. 1173 K by McLaren *et al* (1994), 1273 K by Ellsworth *et al* (1994), at 1373 K by Vance and Anderson (1972), 1323 K by Weber (1991), 1173 K by Colombo and Chrosch (1998b)). Some of these authors might have had problems in the determination of cubic and tetragonal ZrO_2 from x-ray diffraction patterns, and the problem of distinguishing between cubic and tetragonal ZrO_2 has been discussed by Wittels *et al* (1962). We may consider several possible causes discussed below which account for the difference of observations between heavy-ion-irradiated zircon and naturally damaged zircon.

Since natural zircon contains appreciable amounts of trace elements, it is expected that the reaction temperature varies due to these impurities. Effects of impurities on amorphization and annealing were noted in ion-beam irradiation studies of natural monazites (with high impurity contents) and synthetic monazite (Meldrum *et al* 1997b). This may explain the difference in annealing temperature between natural and synthetic zircon samples. The discrepancies may also be due to the nature of the sample forms (bulk versus thin foils) and the type of experiment (high-temperature annealing versus irradiation at high temperature). It is also currently unknown whether there is any possible connection between the phases ZrO_2 and SiO_2 observed while irradiating zircon with heavy ions near 950 K by Meldrum *et al* (1998) and the intermediate phase observed this study which started to appear between 800 K and 900 K.

This issue may be also related to a fundamental and general question: what is the relationship between the structural characteristic of disordered materials and the various physical processes used to produce the amorphous state? Sales *et al* (1990) have reported structural differences between a glass state obtained by thermally quenching melts and ion-beam-amorphized states of lead pyrophosphate. In an EXAFS study of the Zr, Th and U sites in aperiodic/metamict $(Ca,Th)ZrTi_2O_7$ (zirconolite) (Farges *et al* 1993), it was suggested that there are fundamental structural differences in cation environments between radiation-induced aperiodic (metamict) phases and glasses quenched from melts. In a study of electron-irradiation-induced nucleation and growth in $ScPO_4$, Meldrum *et al* (1997a) noted that samples amorphized using 800 keV Kr^{2+} ions were somewhat slower to crystallize under electron irradiation than those treated with 1500 keV Kr^+ ions (requiring $\sim$ 20% higher dose). In a study of ion-bombarded and naturally damaged zircon samples, it was reported that several important similarities and differences exist among ion-irradiated specimens and minerals that undergo radiation damage from α-decay processes (Meldrum *et al* 1999). Therefore, it is also unclear whether the above addressed experimental difference is due to the possible structural differences between the ion-irradiation-induced amorphous state and the α-decay-radiation-induced metamict state.

The observation of five resolved bands between 1050 and 1250 cm^{-1} in sample 157 annealed between 1400 K and 1500 K was unexpected as TEM observations (McLaren *et al* 1994) suggested that the Si-rich phase in decomposed samples was silica glass. These well resolved Raman bands observed in this study appear too sharp to be simply taken as a normal SiO_2 glass. The apparent implication from our observation is that the local structure of the Si-rich phase in this decomposed zircon is probably different from that of SiO_2 glass obtained through quenching melts.

4.4. Intermediate phase

We explain the appearance of additional Raman signals above 800 K as an indication of a structural modification and the formation of an intermediate phase in the corresponding temperature range. This phase is observed mainly in heavily damaged samples at high temperatures (figures 1 and 4) while it could not be detected in untreated zircon. This suggests that this intermediate phase is most likely related to the impact of heating on the damaged parts in metamict zircon. It is unclear whether this phase has the chemical composition of $ZrSiO_4$. However, its characteristic Raman bands near 670, 798 and 1175 cm^{-1} do not match with those of SiO_2 glass in terms of the number of Raman bands and their frequencies (Raman bands of SiO_2 glass at 430, 490, 600, 795, 1059 and 1188 cm^{-1} were observed by Mysen *et al* 1980) and more clearly the strongest Raman band near 430 cm^{-1} in SiO_2 glass due to Si–O bending is absent in this intermediate phase. The lack of the strong characteristic Raman band of cubic ZrO_2 near 607 cm^{-1} (Hirata *et al* 1994) suggests that these additional signals are unlikely to be due to cubic ZrO_2 although tetragonal and monoclinic ZrO_2 are observed at higher temperatures. These extra Raman bands seem due to Si–O vibrations as their frequencies, especially 788 and 1175 cm^{-1}, are too high for interactions between Zr and O. If they are Si–O bands, the 670 cm^{-1} band is likely to be due to Si–O bending while the 798 and 1175 cm^{-1} bands probably due to Si–O stretching. The appearance of these bands, particularly the 670 cm^{-1} band, could indicate a different Si–O–Si linkage. At this stage, there is no clear evidence from the Raman data to rule out or to support the conclusion that this phase is due to decomposition of metamict zircon. Holland and Gottfried (1955) observed in their x-ray data a systematic development and disappearance of an extra peak near 2θ of 35–36.5° with increasing degree of α-decay radiation damage. These authors proposed the formation of an intermediate polycrystalline phase in zircon samples with intermediate dose. It is currently unknown whether there is any possible connection between the intermediate phase proposed by Holland and Gottfried (1955) in unheated samples and the intermediate phase observed this study. Further work by other experimental methods is in progress to understand the nature of the phase observed in our study.

5. Conclusion

The experimental results from this Raman study show that the recrystallization and structure recovery process in damaged zircon through thermal annealing are far more complicated than previous observations have indicated, and that partially and very heavily damaged zircons exhibit significantly different recrystallization processes. The main recrystallization process—the epitaxial growth of crystalline zircon—occurs near 1000 K in partially damaged samples while structural defects in crystalline domains are gradually annealed out at even lower temperatures (starting at 700 K). The lattice recovery is indicated by an increase in the phonon frequencies of the ν_1 and ν_3 Si–O stretching modes and the external band near 357 cm^{-1} together with a sharpening of those phonon bands with increasing annealing temperature.

Heavily damaged zircon tends to decompose into tetragonal ZrO_2 at temperatures around 1125 K and monoclinic ZrO_2 at temperatures above 1600 K. For the highly metamict sample 157 (dose $= 13.1 \times 10^{18}$ α-events g^{-1}), crystalline zircon does not occur until temperatures between 1100 K and 1200 K are reached and a dramatic increase in the intensities of the Raman bands of zircon is observed near 1500 K accompanied by a decrease in the signals of ZrO_2 and SiO_2. This indicates that the $ZrSiO_4$ crystal growth in this metamict sample is associated with the reaction of ZrO_2 with SiO_2.

Extra Raman signals near 670, 798 and 1175 cm^{-1} have been recorded, for the first time, by Raman spectroscopy in heavily damaged samples. These bands start to appear at around 800 K and becomes undetectable in samples annealed above 1400 K. This observation probably suggests the existence of an intermediate phase in this temperature range.

Increasing annealing time does not significantly affect the recrystallization mechanisms and the decomposition process except that it causes changes in the real volumes of the observed different phases. Prolonged isothermal annealing at 1050 K results in a dramatic decrease in the signals due to the intermediate phase and eventually they become undetectable in a sample annealed for 28 days and 8 hours.

Acknowledgments

The authors thank S J B Reed for assistance with the electron microprobe analysis, A Graeme-Barber for assistance with the x-ray diffraction analysis and P Leggo for providing samples UG13 and Moroto used in this study. Financial support from EU network ERB-FMRX-CT97-0108 is gratefully acknowledged.

References

Anastassakis E, Papanicolaou B and Asher I M 1975 *J. Phys. Chem. Solids* **36** 667
Anderson E B, Burakov B E and Vasiliev V G 1993 *Proc. Safe Waste '93* vol 2 p 29
Begg B D, Hess N J, Weber W J, Conradson S D, Schweiger M J and Ewing R C 2000 *J. Nucl. Mater.* at press
Brawer S A and White W B 1975 *J. Chem. Phys.* **63** 2421
Burakov B E 1993 *Proc. Safe Waste '93* vol 2 p 19
Capitani G C, Leroux H, Doukhan J C, Ríos S, Zhang M and Salje E K H 2000 *Phys. Chem. Mineral* at press
Carlone C 1992 *Phys. Rev.* B **45** 2079
Colombo M and Chrosch J 1998a *Radiat. Phys. Chem.* **53** 555
——1998b *Radiat. Phys. Chem.* **53** 563
Colombo M, Chrosch J, Biagini R and Memmi I 1999 *Neues Jahrbuch Mineral.-Monatshefte* 113
Dawson P, Hargreave M M and Wilkinson G F 1971 *J. Phys. C: Solid State Phys.* **4** 240
Ellsworth S, Navrotsky A and Ewing R C 1994 *Phys. Chem. Mineral.* **21** 140
Ewing R C 1994 *Nucl. Instrum. Methods* B **91** 22
——1999 *Proc. Natl Acad. Sci.* **96** 3432
Ewing R C, Lutze W and Weber W J 1995 *J. Mater. Res.* **10** 243
Farges F 1994 *Phys. Chem. Mineral.* **20** 504
Farges F, Ewing R C and Brown G E Jr 1993 *J. Mater. Res.* **8** 1983
Hazen R M and Finger L W 1979 *Am. Mineral.* **64** 157
Hirata T, Asari E and Kitajima M 1994 *J. Solid State Chem.* **110** 201
Holland H D and Gottfried D 1955 *Acta Crystallogr.* **8** 291
Hoskin P W O and Rodgers K A 1996 *Eur. J. Solid State Inorg. Chem.* **33** 1111
Jaeger H, AbuRaddad L and Wick D J 1997 *Appl. Radiat. Isot.* **48** 1083
Keramidas V G and White W B 1974 *J. Am. Ceram. Soc.* **57** 22
Kim D J, Jung H J and Yang I S 1993 *J. Am. Ceram. Soc.* **76** 2106
McLaren A C, Fitz J D and Williams I S 1994 *Geochim. Cosmochim. Acta* **58** 993
Meldrum A, Boatner L A and Ewing R C 1997a *J. Mater. Res.* **12** 1816
——1997b *Phys. Rev.* B **56** 13 805
Meldrum A, Boatner L A, Zinkle S J, Wang S X, Wang L M and Ewing R C 1999 *Can. Mineral.* **37** 207
Meldrum A, Zinkle S J, Boatner L A and Ewing R C 1998 *Nature* **395** 56
Murakami T, Chakoumakos B C, Ewing R C, Lumpkin G R and Weber W J 1991 *Am. Mineral.* **76** 1510
Mursic Z, Vogt T, Boysen H and Frey F 1992a *J. Appl. Crystallogr.* **25** 519
Mursic Z, Vogt T and Frey F 1992b *Acta Crystallogr.* B **48** 584
Mysen B O, Virgo D and Scarfe C M 1980 *Am. Mineral.* **65** 690
Nasdala L, Irmer G and Wolf D 1995 *Eur. J. Mineral.* **7** 471
Nicola H H and Rutt H N 1974 *J. Phys. C: Solid State Phys.* **7** 1381

Sales B C, Ramey J O, McCallum J C and Boatner L A 1990 *J. Non-Cryst. Solids* **126** 179
Salje E K H, Chrosch J and Ewing R C 1999 *Am. Mineral.* **84** 1107
Siu G G, Stokes M J and Liu Y 1999 *Phys. Rev.* B **59** 3173
Smith D K and Newkirk H K 1965 *Acta Crystallogr.* **18** 982
Stott V H and Hilliard A 1946 *Mineral. Mag.* **27** 198
Syme R W G, Lockwood D J and Kerr H J 1977 *J. Phys. C: Solid State Phys.* **10** 1335
Vance E R 1975 *Radiat. Eff.* **24** 1
Vance E R and Anderson B W 1972 *Mineral. Mag.* **38** 605
Vaz J E and Senftle F E 1971 *J. Geophys. Res.* **76** 2038
Weber W J 1991 *Radiat. Eff. Defects Solids* **115** 341
——1993 *J. Am. Ceram. Soc.* **76** 1729
Weber W J, Ewing R C and Lutze W 1996 *Mater. Res. Soc. Symp. Proc.* vol 412 (Pittsburgh, PA: National Research Society) p 25
Williford R E, Devanathan R and Weber W J 1998 *Nucl. Instrum. Methods* B **141** 94
Wittels M C, Steigler J O and Sherrill F A 1962 *J. Nucl. Energy* A/B **16** 237
Zhang M, Salje E K H, Farnan I, Graeme-Barber A, Daniel P, Ewing R C, Clark A M and Leroux H 2000 *J. Phys.: Condens. Matter* **12** 1915